TECHNICAL PAPER

Dynamic Response Analysis of Ballasted Railway Track–Ground System under Train Moving Loads using 3D Finite Element Numerical Modelling

Md. Abu Sayeed[1] · Mohamed A. Shahin[2]

Abstract

The faster and heavier trains in modern railway traffic are getting popularity in the public transportation authorities of many countries. Such trains cause higher stresses and excessive deformations in the ballasted railway track substructure under train dynamic loadings, which raises the risk of track damage and derailment. It is thus essential to investigate the impact of different influencing factors on the dynamic response of ballasted railway track–ground systems. In this study, a sophisticated three-dimensional finite element model simulating realistic train moving loads is presented and used to investigate the dynamic response of ballasted railway tracks in terms of stress transmission and track deflections under various train–track–ground conditions. The influencing factors considered in this study include the modulus and thicknesses of track substructure layers, the amplitude of train moving loads and the train speed. The outcomes of this study encompass important guidance to railway engineers to assist in finding the best possible scheme for the design of ballasted railway tracks and lifetime maintenance.

Keywords Ballasted railway tracks · Finite element method · Numerical modelling · Train moving loads · Railway track response

✉ Mohamed A. Shahin
M.Shahin@curtin.edu.au

Md. Abu Sayeed
MdAbuSayeed@ce.ruet.ac.bd

1 Department of Civil Engineering, Rajshahi University of Engineering & Technology (RUET), Rajshahi 6204, Bangladesh

2 School of Civil and Mechanical Engineering, Curtin University, Bentley, WA 6845, Australia

1 Introduction

In recent years, modern high-speed trains (HSTs) have become the most popular means of public transportation in many countries around the world due to the high demand for safer and faster vehicles. To run HSTs, new challenges and problems related to the performance of rail track foundations arise, primarily due to the significant amplification effects of the track–ground vibrations. The dynamic loads of HSTs, as well as heavy axle loads, produce higher stresses in the railway track substructure layers, causing excessive deformations (Xu et al. 2018) and raising the risks of train operation, especially at the critical velocity, i.e. the train speed that creates a resonant-like problem (Alves Costa et al. 2015; Krylov et al. 2000; Madshus and Kaynia 2000). To prevent the operational risks and meet the demand for faster trains, an investigation of the dynamic behaviour of the track–ground system under true train moving loads has become a key research issue.

During train movement, the track substructure elements/layers become subjected to complex train induced cyclic loading with principal stress rotation (Dareeju et al. 2017; Gräbe and Clayton 2009; Powrie et al. 2007), which may significantly affect track response and the corresponding deformations (Inam et al. 2012; Qian et al. 2019). However, most of the previous existing analytical and theoretical models used for the design of railway tracks, such as GEOTRACK(Chang et al. 1980) and KEN-TRACK (Huang et al. 1987) are plagued by several limitations including the inability to simulate the true dynamic effects of train-induced loads. To overcome such shortcomings, numerous research efforts based on finite element method (FEM) and boundary element method (BEM), which are eased by advanced computer processors, have been performed in the last few years and have achieved some degree of success (e.g. Alves Costa et al. 2012, 2015; Bian et al. 2014; El Kacimi et al. 2013; Galavi and Brinkgreve 2014; Kouroussis et al. 2011a, b; Mezeh et al. 2021; Sayeed and Shahin 2016a, b; Shih et al. 2016; Sun et al. 2020; Takemiya 2003; Wang et al. 2020; Yang et al. 2009). However, to this end, only a few studies have been able to simulate the actual dynamic/cyclic behaviour of ballasted railway track–ground system under true train moving loads. On the other hand, to evaluate the effect of train speed on the ballasted railway track–ground system, most of the aforesaid studies only counted a single wheel moving load or a single cyclic loading on a specified point of the track rather than the whole train moving loads. Thus, the role of the principal stress rotation on the behaviour of track soil substructure was usually ignored. Moreover, the consideration of a single wheel moving load is highly arguable as the dynamic intensification and critical velocity depend on the actual loading regime of a complete running train, which combine a series of wheel loads of different amplitudes and geometry (hence the role of frequency). Therefore, the real train geometry (distance between the axles and bogies of the car) and the amount of discrete axle load need to be considered in the analysis of the effect of train speed.

In this study, a sophisticated three-dimensional (3D) finite element (FE) model previously developed and validated by the authors (i.e. Sayeed and Shahin 2016a, b) is used to investigate the influence of some important factors on the performance of the track–ground system under true train moving loads, including the

stiffness and thickness of the track substructure layers (ballast and subgrade), train loading amplitude and train speed. The obtained results are essentially ana-lysed and discussed, and the outcomes provided some useful directions to railway engineers to find the best possible strategy for the design and maintenance of bal-lasted railway tracks.

2 Numerical Modelling of Ballasted Railway Track

To analyse the dynamic responses of ballasted railway track–ground system under train moving loads, a numerical modelling-based software GTS-NX (MIDAS IT. Co. Ltd. 2013) is utilised to develop a three-dimensional (3D) finite element (FE) model. Figure 1 presents the 3D FE model that is used to simulate the dynamic behaviour of ballasted railway track–ground system. This model is similar (but with a more simple substructure condition) to that used previously (Sayeed and Shahin 2016a, b) to simulate the practical deformation behaviour of railway track at the Ledsgard site. The length of the modelled track in *X*-, *Y*- and *Z*-directions are 36 m, 80 m and 7.5 m, respectively. The rails are modelled using one-dimensional (1D) linear elastic beam elements along the *Y*-direction. A UIC-60 (I- shaped) section is modelled for the rail, which is fixed to the sleepers by rail pads. The rail pads are characterised using elastic link elements and the other track components are modelled using 3D solid elements. The sleepers are placed in the transverse direction of the rail at 0.6 m spacing. The sleepers and subgrade are modelled as linear elastic (LE) materials, while the granular ballast layer is modelled as elastoplastic Mohr–Coulomb (MC) material. It should be noted that due to the lack of information about the plasticity

Fig. 1 Three dimensional FE model of track–ground system (**a**) cross section of the model (not to scale); (**b**) 3D view of the model
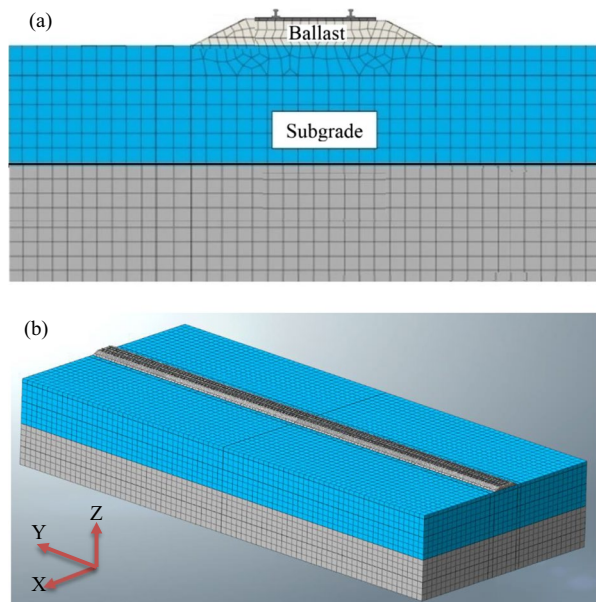
characteristics of the subgrade soil and to reduce the simulation time, the subgrade layer is assumed to be elastic in the current model. This assumption is reasonable and should not affect the overall results because the thickness of the granular ballast layer is usually selected so that the level of stress applied on top of the subgrade layer is low; hence, no (or only a small) zone of plastic yielding can be developed in the subgrade. The properties of the materials used in the 3D FE model are summarised in Table 1.

In any dynamic FE analysis, the mesh size of finite elements, model size and model boundaries should be selected correctly to confirm the precision of the results (Shih et al. 2016). In the current model, the FE mesh element size is estimated based on the smallest wavelength that allows the high-frequency motion to be simulated correctly. As such, the dimensions of the 3D solid elements are selected to be: 0.17 m×0.14 m×0.20 m for the sleepers; 0.20 m×0.20 m×0.20 m for the ballast; and 0.60 m×0.60 m×0.60 m for the subgrade. The viscous dampers are linked to the vertical boundaries to absorb the incident p-waves and s-waves, and thus characterise infinite boundary conditions, as recommended by several scholars (e.g. Kouroussis et al.

Table 1 Material properties used in the three dimensional FE model (Sayeed and Shahin 2018)

Track component	Material property	Value
Rail	Dynamic modulus of elasticity, E (MPa)	210,000
	Poisson's ratio, ν	0.30
	Moment of inertia, I (m^4)	3.04×10^{-5}
Sleeper	Dynamic modulus of elasticity, E (MPa)	30,000
	Poisson's ratio, ν	0.20
	Unit weight, γ (kN/m^3)	20.2
	Length, l (m)	2.50
	Width, w (m)	0.27
	Thickness (m)	0.20
Ballast	Dynamic modulus of elasticity, E_b (MPa)	270
	Poisson's ratio, ν	0.30
	Unit weight, γ (kN/m^3)	17.3
	Cohesion, c (kPa)	0.00
	Friction Angle, ϕ°	50.0
	Thickness, H_b (m)	0.45
	Shear wave velocity, C_s (m/s)	243
	Damping ratio, ξ	0.03
Subgrade	Dynamic modulus of elasticity, E_s (MPa)	60.0
	Poisson's ratio, ν	0.35
	Unit weight, γ (kN/m^3)	18.8
	Thickness, H_s (m)	7.50
	Shear wave velocity, C_s (m/s)	108
	Raleigh wave velocity, C_R (m/s)	101
	Damping ratio, ξ	0.03

Fig. 2 Simulation of moving loads (Araújo 2011)
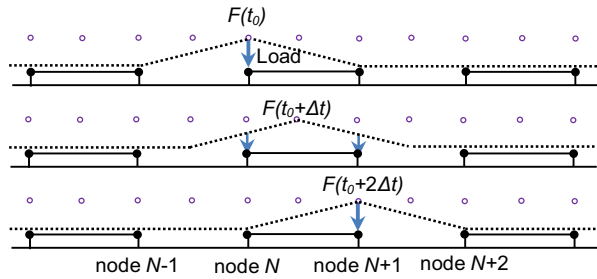
Table 2 Geometry and axle loads of the X-2000 HST (Takemiya 2003)

Car number, n	Spacing			Standard wheel load	
	L_a (m)	L_b (m)	L_c (m)	P_F(kN)	P_B (kN)
1	2.9	14.5	22.2	81.0	61.3
2	2.9	17.7	24.4	61.3	61.3
3	2.9	17.7	24.4	61.3	61.3
4	2.9	17.7	24.4	61.3	61.3
5	2.9	9.5	17.2	90.0	90.0

2011a, b). To simulate hard rock conditions at the trackbed, all nodes at the lowermost boundary are set to be fixed in all directions. The material damping of the FE model is characterised by the mass and stiffness proportional coefficients, using the Rayleigh damping which is usually utilised for the dynamic analyses (Ju and Ni 2007). During the moving load simulation, the time step is chosen based on the Courant number (Galavi and Brinkgreve 2014) and its value is always considered to be less than one.

In this study, the simulation of the train moving loads is performed according to Araújo (2011). In such a simulation, the FE rail nodes (denoted as *loading nodes*) are firmly linked to the sleepers that are subjected to a cyclic wheel load. The moving loads can be characterised by triangular pulses distributed among three consecutive loading nodes along the *Y*-direction of the FE model. As shown in Fig. 2, when the wheel departs the preceding node, *N*, the amplitude of the wheel load, *F*, increases at the loading node $N+1$. The amplitude becomes the peak value once the wheel is directly above that loading node $N+1$, then finally decreases back to zero when the wheel arrives at the subsequent node $N+2$. Thus, the triangular pulse travels the distance between two consecutive loading nodes by a time interval equivalent to the spacing between the two loading nodes divided by the train speed, *C*. For instance, if the speed of the train is 108 km/h (i.e. 30 m/s) and the distance between two loading nodes is 0.6 m, then the wheel will travel from one loading node to another in 0.02 s. Likewise, a series of train wheels representing the X-2000 HST is simulated along the railway track at a train speed of 30 m/s, unless otherwise specified. The standard wheel loads and train geometry of the X-2000 HST are given in Table 2, which includes (for each car) the wheel to wheel distance (L_a), bogie to bogie distance (L_b), car length (L_c), fore-wheel load (P_F) and back wheel load (P_B). A schematic illustration of the X-2000 passenger train is shown in Fig. 3.
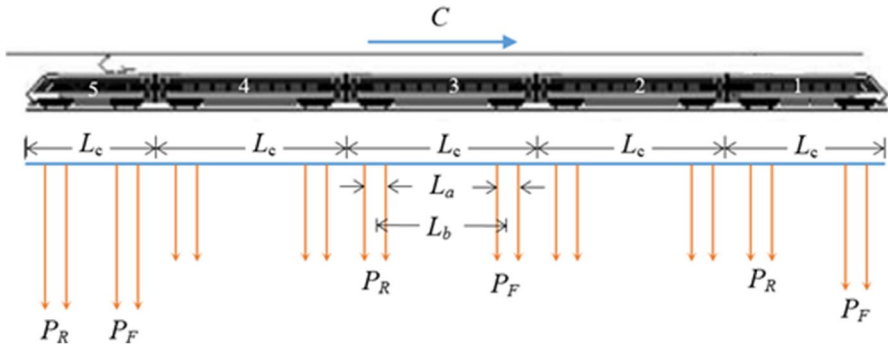
Fig. 3 Geometry of the X-2000 HST (Takemiya 2003)

3 Stress Analysis

The accurate calculation of the distribution of deviatoric stress in the track–ground system under true train moving loads is a very important factor for the design of ballasted railway track foundations. Consequently, this part of the paper is dedicated to calculating the deviatoric stress distribution in the track–ground system using the developed 3D FE model. The deviatoric stress is defined as follows:

$$\sigma_d = \sqrt{1/2[(\sigma_1 - \sigma_2)^2 + (\sigma_2 - \sigma_3)^2 + (\sigma_3 - \sigma_1)^2]}$$

where σ_1, σ_2 and σ_3 are the principal stresses, and when $\sigma_2 = \sigma_3$, then $\sigma_d = \sigma_1 - \sigma_3$.

In general, the peak deviatoric stresses in the ballast and subgrade layers develop along the rail beneath the sleeper bed rather than the crib, and the peak deviatoric stress at any distance beneath the sleeper bed develops at the sleeper end (Sayeed and Shahin 2018). Hence, for design purposes, the deviatoric stresses in the track substructure layers (ballast and subgrade) are calculated beneath the sleeper end, which represents the maximum induced deviatoric stress zone. In the deviatoric stress analyses, the material properties given in Table 1 are considered to remain the same, unless otherwise specified.

### 3.1 Influence of Stiffness of Track Substructure Layers

In this section, the impacts of stiffness (i.e. dynamic modulus of elasticity) of track substructure layers (ballast and subgrade) on the distribution of deviatoric stress with depth are explored. Herein, the track properties given in Table 1 are kept the same except that a stiff ballast layer is represented by a dynamic elastic modulus of 540 MPa, while a soft ballast layer is accounted for by a dynamic elastic modulus of 135 MPa. Likewise, a dynamic elastic modulus of 120 MPa is used to characterise a stiff subgrade, whereas a dynamic elastic modulus of 15 MPa is utilised to represent a soft subgrade. It should be noted that the ranges of the above-mentioned dynamic elastic modulus for both the ballast and subgrade are selected carefully to reflect the

practical ranges expected in major railway tracks, as recommended by Li (1994) and Li and Selig (1994).

3.1.1 Distribution of Deviatoric Stress in Ballast Layer

The influence of the ballast layer stiffness on the deviatoric stress response within the ballast layer is demonstrated in Fig. 4. For all ballast conditions (i.e. E_b = 135, 270 and 540 MPa), the deviatoric stress at the ballast surface changes with time when the train moving load crosses the point of concern, and the deviatoric stress amplitude reaches the peak while the maximum wheel load is just above the measuring point (Fig. 4a). It is worth mentioning that the deviatoric stress developed at the ballast surface increases with the increase in the ballast stiffness or dynamic elastic modulus. On the contrary, it can be observed from Fig. 4b that for all ballast modulus, the deviatoric stress reduces with the depth of the ballast layer. It is also observed that the stress dissipation rate is not the same; it is less for the soft ballast.

Fig. 4 Influence of ballast modulus on the deviatoric stress response of the ballast layer for soft subgrade
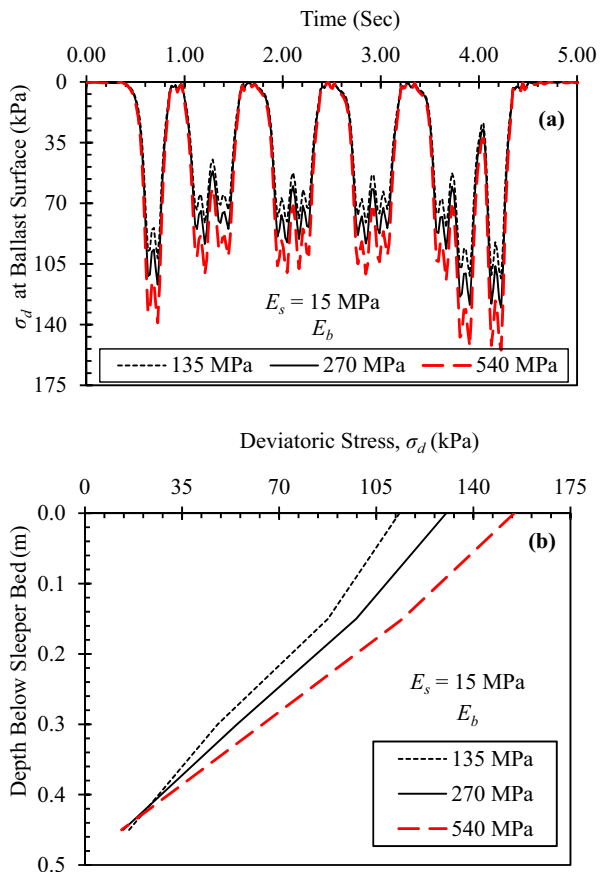
To examine the effect of the subgrade layer stiffness on the deviatoric stress response, four separate values of the subgrade dynamic elastic modulus are selected (i.e. E_s = 15 MPa, 30 MPa, 60 MPa and 120 MPa). Figure 5 illustrates the influence of the subgrade stiffness on the deviatoric stress distribution within the ballast layer. It can be observed from Fig. 5a that with the rise of the subgrade layer stiffness, the deviatoric stress developed at the ballast surface decreases significantly. It is noted that substantial stress is developed in the ballast layer when it is supported by a soft subgrade, which might increase the ballast particle breakage and ballast fouling. It is also apprehended that the ballast layer has greater efficiency in distributing the stress when it is supported by a soft subgrade (see Fig. 5b).

The dual influence of the stiffness of the subgrade and ballast on the deviatoric stress distribution with the ballast layer is illustrated in Fig. 6. It can be observed that the utmost deviatoric stress arises in the ballast surface for the dual effect of a soft subgrade and stiff ballast. It can also be noted that, with the decrease in the subgrade stiffness and the increase in the ballast stiffness, the stress spreading efficiency within the ballast layer increases, and vice is versa.

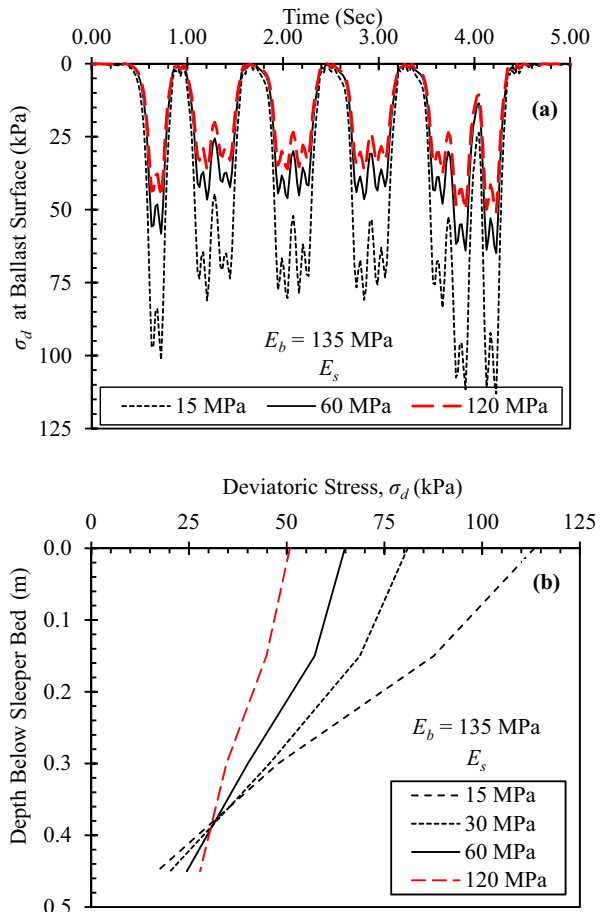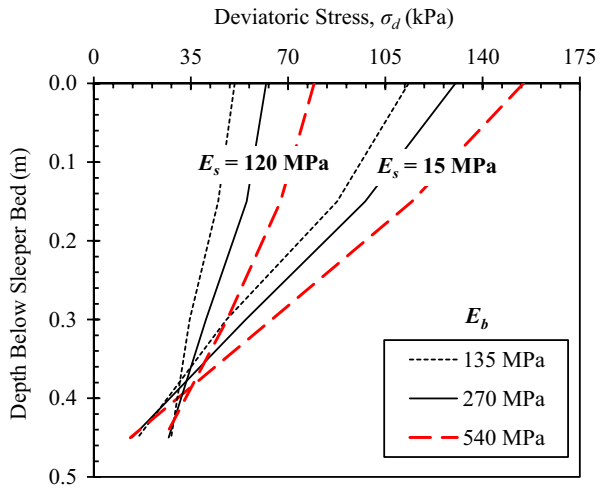**Fig. 5** Influence of subgrade modulus on the deviatoric stress response of the ballast layer

Fig. 6 Influence of combined effects of stiffness of ballast and subgrade on the deviatoric stress distribution of the ballast layer

### 3.1.2 Distribution of Deviatoric Stress in Subgrade Layer

Figure 7 shows the influences of ballast stiffness on the deviatoric stress distribution with the subgrade layer. It can be seen that the induced deviatoric stress at the subgrade surface decreases with the increase in the ballast modulus, for both the soft and stiff subgrade soils. Conversely, the dissimilarity of the deviatoric stress at each depth below the sleeper bed reduces with the depth of track substructure and becomes very small at about 5 m for the soft subgrade condition (Fig. 7a). However, the discrepancy of the deviatoric stress at each depth below the sleeper bed caused by different ballast stiffness continues with depth for the stiff subgrade condition (Fig. 7b).

The deviatoric stress behaviour in the subgrade layer due to its stiffness effect is depicted in Fig. 8. It is realised that the deviatoric stress at the subgrade surface intensifies with the rise of the subgrade stiffness (Fig. 8a). On the contrary, the variation in the deviatoric stress at each depth of the subgrade layer (due to its stiffness variation) decreases with the depth below the sleeper bed (Fig. 8b).

3.2 Influence of Ballast Layer Thickness

The influence of the ballast layer thickness, H_b, on the deviatoric stress distribution with the subgrade layer is examined assuming a range of ballast layer thickness varying from 0.15 m to 1.35 m. Figure 9 presents the deviatoric stress distribution with the depth of the subgrade layer for different ballast layer thicknesses. It can be seen that the deviatoric stress at the top surface of the subgrade (i.e. just beneath the ballast layer) decreases significantly with the increase in the ballast layer thickness irrespective of the subgrade stiffness. It can also be observed from Fig. 9a that there is a noteworthy difference in the deviatoric stress at the same depth for the soft subgrade layer; however, such a difference reduces with the depth below the sleeper bed. On the other hand, the difference in the deviatoric stress at the same depth below the sleeper bed is almost insignificant for the stiff subgrade layer (Fig. 9b).

Fig. 7 Influence of ballast modulus on deviatoric stress distribution with the depth of the subgrade layer for (**a**) soft subgrade; and (**b**) stiff subgrade condition
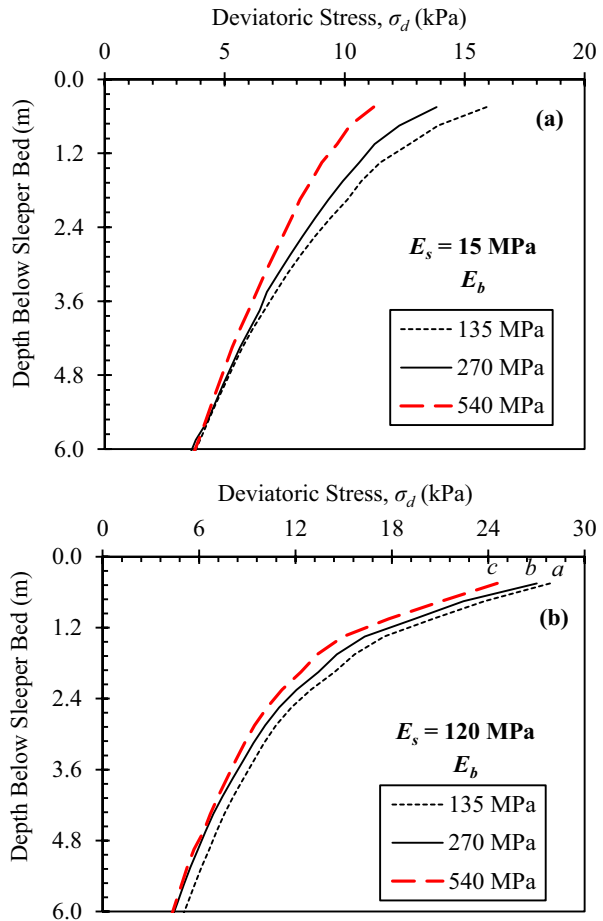
In real situations, the rise of the ballast layer thickness reduces the deviatoric stress in the subgrade layer in double ways. Primarily, the distance between the sleeper bed and the subgrade surface inevitably increases with the increase in the ballast layer thickness. As a result, the induced deviatoric stress at the subgrade surface (i.e. below the bottom of the ballast layer) is decreased by the stress distribution effect. Moreover, the larger stiff ballast layer thickness spreads the train moving loads in more areas and thus decreases the deviatoric stress in the subgrade layer. Conversely, when there is a minor difference between the modulus of the ballast layer and the subgrade layer, the second effect fades. Therefore, the influence of the ballast layer thickness on the deviatoric stress distribution in the subgrade becomes minor.

3.3 Influence of Subgrade Layer Thickness

The influence of the subgrade layer thickness on the deviatoric stress distribution within the subgrade is examined by considering three particular subgrade

Fig. 8 Influence of subgrade modulus on deviatoric stress distribution with the depth of the subgrade layer for soft ballast condition
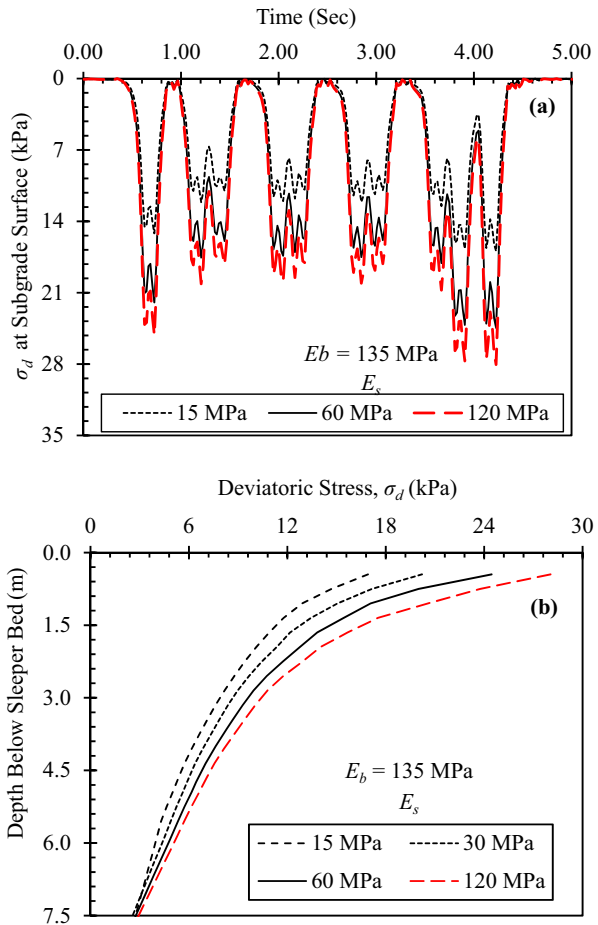
thicknesses (i.e. $H_s = 3.5$ m, 7.5 m and 10 m) overlying the hard rock. Figure 10 shows the distribution of the deviatoric stress for the three subgrade thicknesses considered. It can be seen that there is a negligible dissimilarity in the deviatoric stress at each depth of the subgrade, except at the interface of the subgrade with the hard rock. Since the effect of the subgrade thickness on the distribution of the deviatoric stress in the subgrade is insignificant, the subgrade thickness is assumed to be fixed at 7.5 m in all of the following deviatoric stress analyses performed until otherwise informed.

3.4 Influence of Amplitude of Train Moving Loads

To investigate the influence of the amplitude of train moving loads on the distribution of deviatoric stress in the track substructure layers, four distinct loading

Fig. 9 Influence of ballast layer thickness on deviatoric stress distribution with the depth of the subgrade layer for (**a**) soft subgrade; and (**b**) stiff subgrade
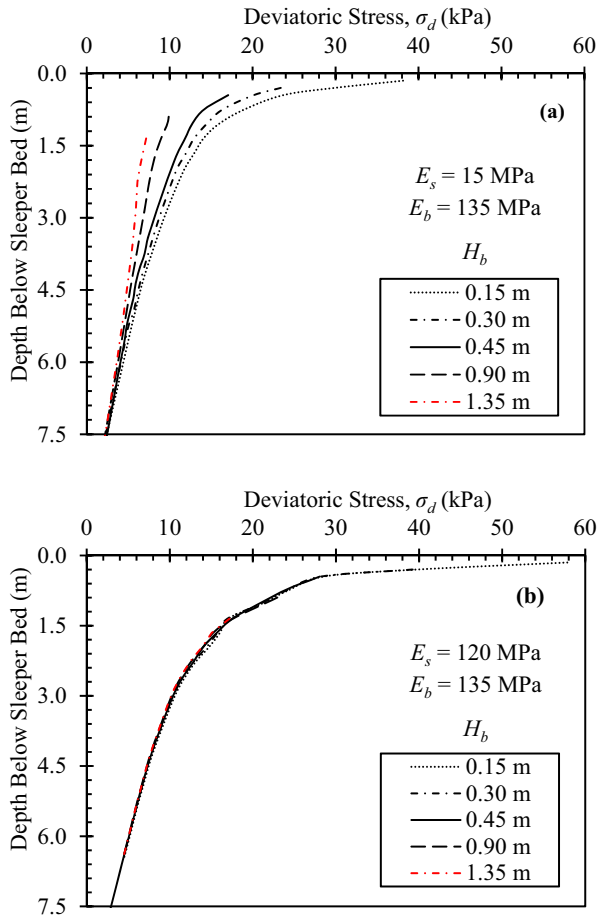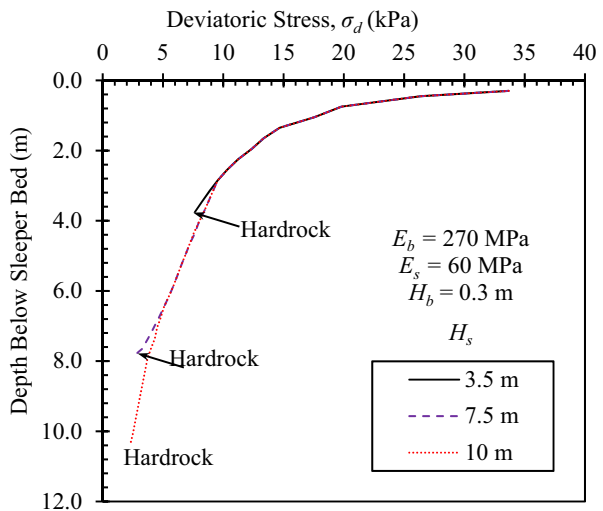

Fig. 10 Influence of subgrade layer thicknesses on deviatoric stress distribution in the subgrade layer

amplitudes (i.e. 75%, 100%, 150% and 200%) typical to the wheel loads of the X-2000 HST (see Table 2) are considered and the results are depicted in Fig. 11. It can be seen that the deviatoric stress in both the ballast and subgrade layers rises proportionately with the rise of the amplitude of the wheel loading. The combined effect of the subgrade stiffness and different amplitudes of train loading on the ballast surface deviatoric stress and subgrade surface deviatoric stress is shown in Fig. 12. It can be observed that both the ballast surface deviatoric stress and subgrade surface deviatoric stress are proportionate to the loading amplitude for all subgrade conditions.

4 Deformation Analysis

The time history track deflection responses of different ballast and subgrade stiffnesses are illustrated in Fig. 13. It can be seen that for all ballast modulus and subgrade modulus, the track deflection occurs when the wheel crosses the point

Fig. 11 Influence of amplitude of train moving load on deviatoric stress distribution of (**a**) ballast layer; and (**b**) subgrade layer
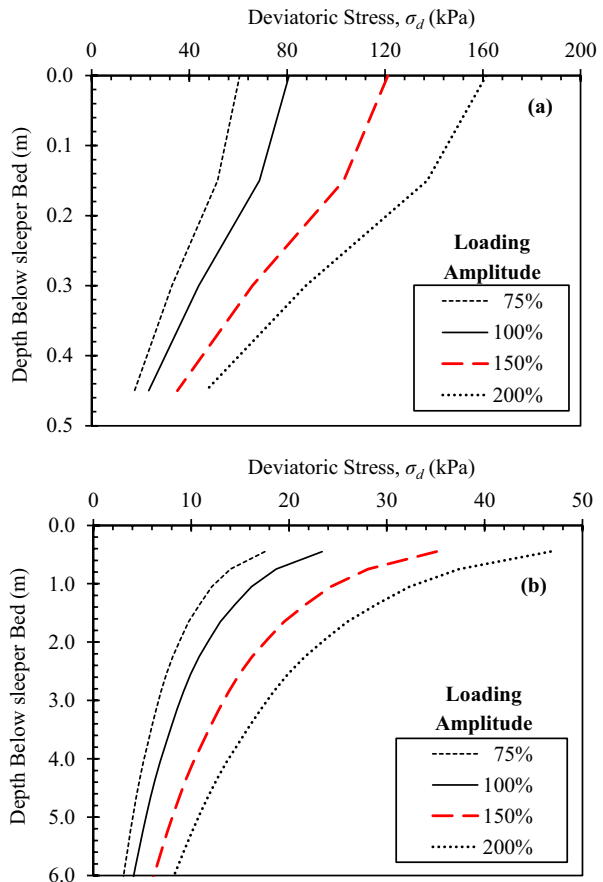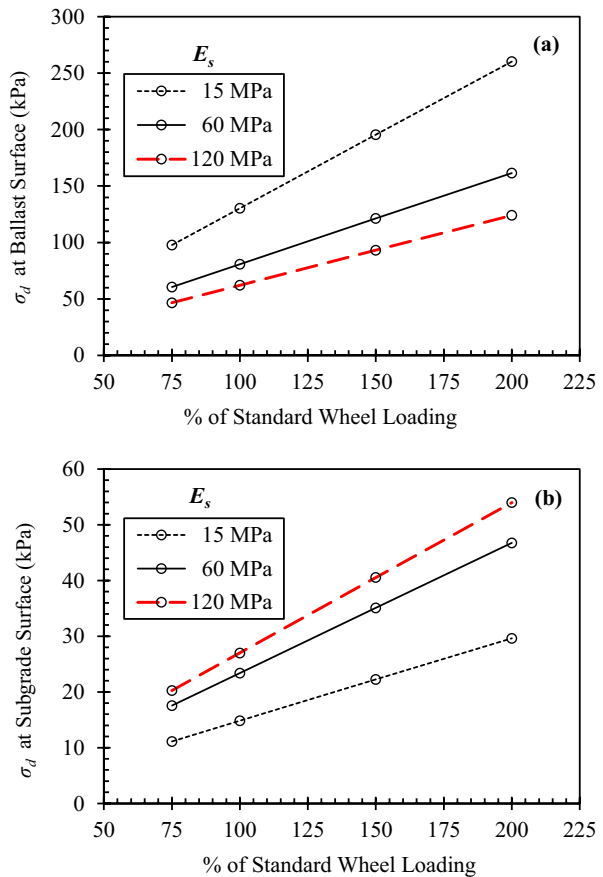
Fig. 12 Relationship between loading amplitude and deviatoric stress at (a) ballast surface; and (b) subgrade surface

of concern in a similar way to the results presented earlier in Fig. 4a. Further, the increase in both the ballast modulus and subgrade modulus decreases the track deflection. However, it is noted that the variation of the track deflection is negligible when the ballast modulus varies from 270 to 540 MPa (Fig. 13a). On the contrary, there is a significant difference in the track deflection when the subgrade modulus increases from 15 to 120 MPa (Fig. 13b).

Figure 14 illustrates the time history track deflection responses of different thicknesses of ballast and subgrade layers. It can be seen that the time history track deflection responses for all ballast and subgrade thicknesses are very similar to the results presented above in Fig. 13. Additionally, the track deflection reduces with the increase in the ballast thickness (Fig. 14a). On the contrary, the track deflection increases with the increase in subgrade layer thickness, although the difference is negligible when the subgrade thickness increases from 7.50 to 15.0 m (Fig. 14b). Since the deviatoric stress at a depth of 7.5 m or more of the subgrade layer is approximately 10% of the subgrade surface deviatoric stress (see Fig. 10); the difference in the track deflections become negligible.

Fig. 13 Time history track deflection response for different: (**a**) ballast modulus; and (**b**) subgrade modulus
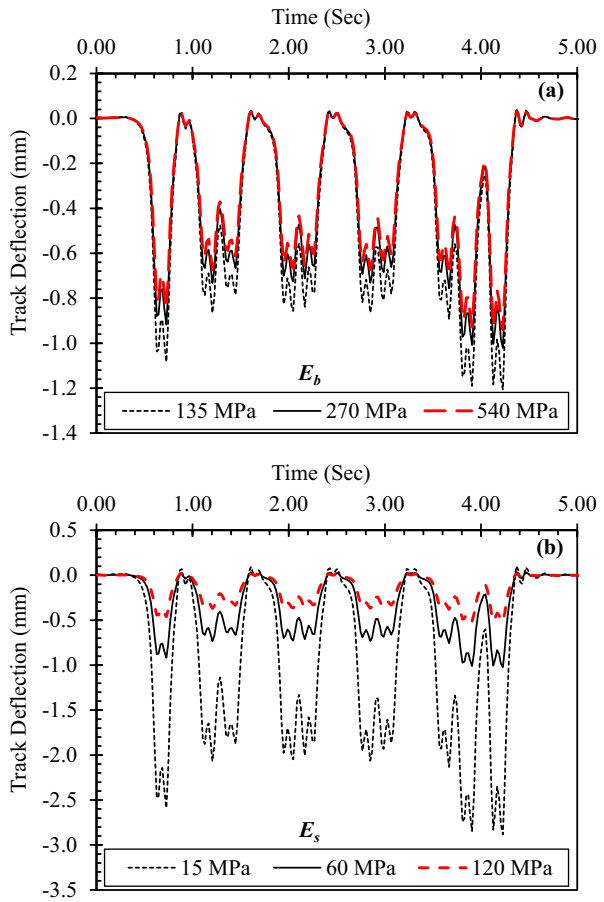
The time history track deflection responses of different train loading amplitudes are illustrated in Fig. 15. It can be observed that the track deflection rises proportionately with the rise of the loading amplitude.

The above results summarise that the presence of a soft subgrade layer and heavy wheel loading with the absence of a proper stiff ballast layer thickness has a significant effect on the deviation of the ballasted railway track, which can derail the railway track.

5 Influence of Train Speed

As stated previously, train speed is a key factor that affects track performance. Therefore, in this section, the effects of train speed on the railway track performance are investigated under various subgrade conditions. Figure 16 shows the track vertical deflections versus train speed for a track subgrade modulus of 15 MPa. It can be

Fig. 14 Time history track deflection response for different thicknesses of (**a**) ballast layer; and (**b**) subgrade layer
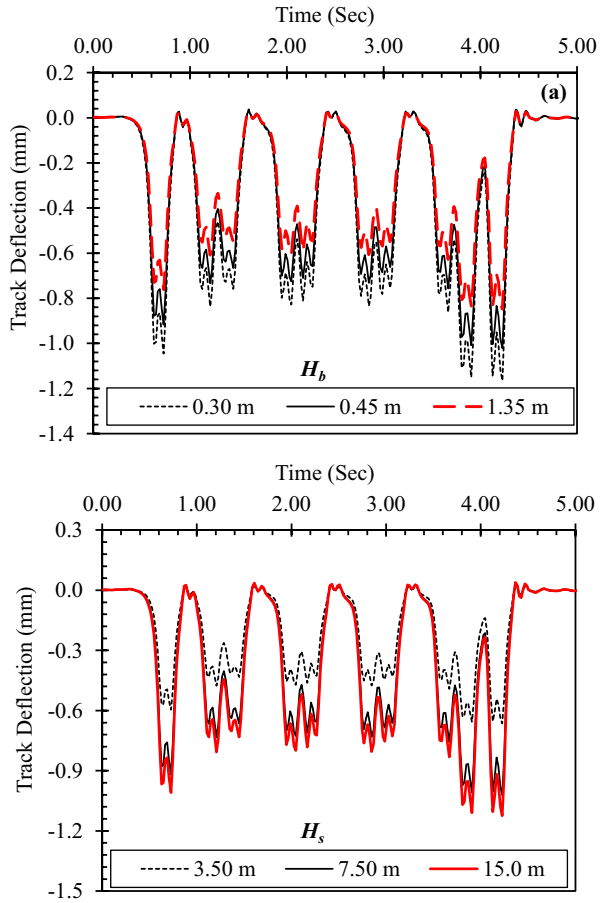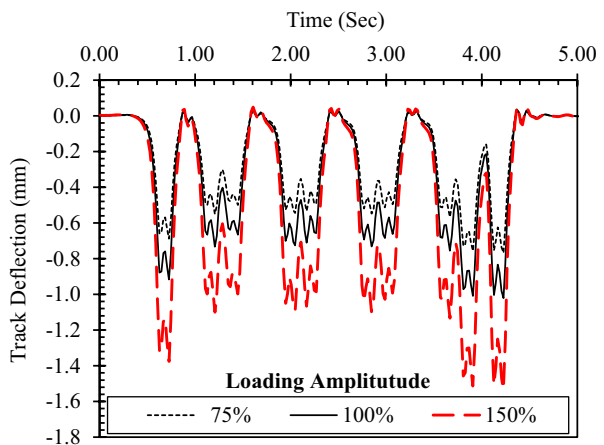

Fig. 15 Time history track deflection response for different train load amplitudes

observed that the sleeper vertical deflection usually increases with the increase in the train speed, reaching its peak value at the critical velocity before it drops with a further rise in the train speed. As can be seen, the critical velocity is found to be 92 m/sec, which is higher than the Rayleigh wave velocity of the top subgrade soil ($C_R = 50.5$ m/s) overlying the hard rock. This advises that the critical velocity is not always identical to the Rayleigh wave velocity of the upper subgrade soil as is sometimes assumed, and this can be credited to the existence of the bottom solid hard rock layer. These findings are consistent with the results reported by Bian et al. (2014) and Alves Costa et al. (2015) in the qualitative sense.

Most of the existing design methods generally consider the impact of train speed by simply utilising numerous empirical formulations that overlook the characteristics of the subgrade conditions. However, the propagation wave velocity of any soil medium is highly dependent on its stiffness and thickness (Alves Costa et al. 2012, 2015). Therefore, the influence of the top subgrade stiffness (or soil modulus), E_s, and thickness, H_s, on the critical velocity of the train needs to be investigated. Accordingly, four different values of subgrade modulus (i.e. $E_s = 7.5$, 15, 30 and 120 MPa) and three thicknesses of the top subgrade (i.e. $H_s = 5$, 7.5 and 10 m) are considered in this investigation. The results are presented in Fig. 17 in terms of the relationship between the speed impact factor (SIF) and the corresponding train speed. The SIF is defined as the ratio of the highest dynamic vertical sleeper deflection at a particular train speed to the highest sleeper vertical deflection at quasi-static condition (i.e. sleeper deflection at a very small train speed of 5 m/s) for different subgrade thickness and stiffness.

It is observed that, for all values of H_s and E_s, the SIF rises with the rise of train speed until it reaches a peak value at the critical velocity, after which it falls with a further rise of the train speed. It is also observed that the amplitude of the SIF decreases with the increase in both the subgrade stiffness and thickness. On the other hand, the magnitude of the critical velocity increases with the increase in the subgrade stiffness, while it decreases with the increase in the subgrade thickness. The practical implication of this finding is that the localised ground improvement

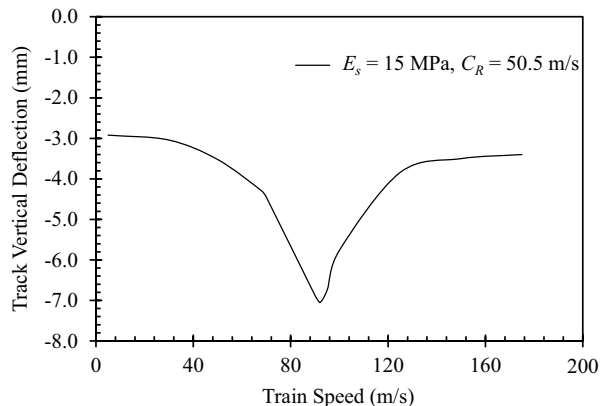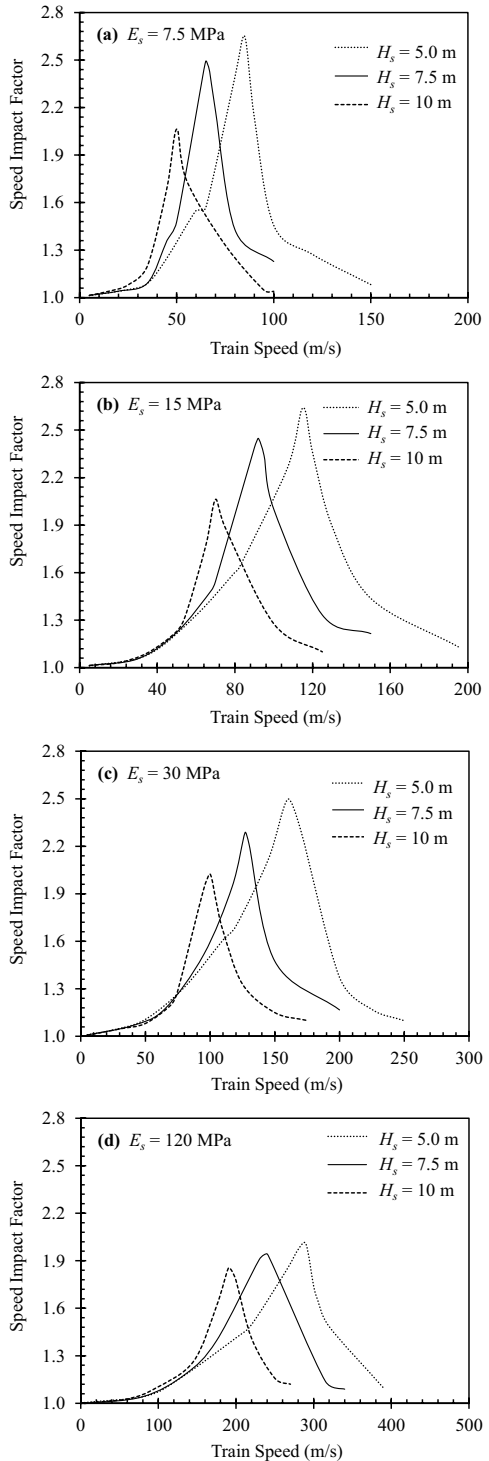**Fig. 16** Variation of peak track vertical deflection with train speed

Fig. 17 Variation of speed impact factor with train speed under different subgrade conditions and train speed impact factor

of the soft subgrade can be very beneficial in decreasing the SIF and increasing the critical velocity of trains.

6 Conclusions

In this paper, the deviatoric stress transmission and distribution in the railway track substructure layers and the corresponding track deflections are investigated carefully using an advanced three-dimensional finite element modelling under true train moving loads for numerous train–track–ground conditions. The factors considered in the analysis include the stiffness (modulus) and thicknesses of the ballast and subgrade layers, in addition to the amplitude of train loadings and train speed. The following verdicts are obtained from the results achieved in the current study:

- The ballast modulus and subgrade modulus both affect the deviatoric stress distribution in the ballast layer significantly. The supreme deviatoric stress arises in the ballast surface for the duel effects of the soft subgrade and stiff ballast condition, which might progress the breaking of the ballast particles causing ballast fouling. Additionally, with the decrease in the subgrade modulus and increase in the ballast modulus, the effect of stress distribution in the ballast layer increases, and vice is versa.
- The deviatoric stress at the subgrade surface reduces with the rise of ballast stiffness irrespective of the subgrade condition. However, an increase in the subgrade stiffness increases the deviatoric stress of the subgrade layer.
- Due to the difference in ballast modulus, the dissimilarity in the deviatoric stress at any depth below the sleeper bed reduces with depth and becomes insignificant after about 5 m depth for the soft subgrade case. Conversely, for the stiff subgrade condition, the dissimilarity in the deviatoric stress remains significant even after about 6 m depth.
- In general, a rise in the ballast layer thickness considerably reduces the deviatoric stress in the subgrade layer. Besides, for the soft subgrade, there is a remarkable dissimilarity in the deviatoric stress with depth due to the difference in the ballast layer thickness; however, such a dissimilarity is almost negligible in the stiff subgrade condition and for different subgrade thicknesses.
- An increase in the wheel loading rises the deviatoric stress proportionately in both the ballast and subgrade layers irrespective of the track conditions. Consequently, the track deflection rises proportionately with the rise of the train wheel loading.
- The track deflection decreases with the increase in both the ballast modulus and subgrade modulus. In addition, the track deflection reduces with the rise of the ballast layer thickness. Conversely, the track deflection rises with the increase in the subgrade layer thickness. Thus, the lack of stiff ballast layer thickness with the presence of excessive soft subgrade layer thickness and heavy wheel loading have significant effects on the track deflection, which may cause railway track failure or derailment.

- The subgrade stiffness and thickness significantly influences the speed impact factor (SIF) and critical velocity of the train. The SIF is found to decrease with the increase in both the subgrade stiffness and thickness. Conversely, with the increase in the subgrade stiffness, the amplitude of critical velocity increases, while it decreases with the increase in the subgrade thickness.

Data availability Not Applicable.

Code availability Not Applicable.

Declarations

Conflicts of interest/Competing interests Not Applicable.

References

Alves Costa, P., Calçada, R., Silva Cardoso, A.: Track-ground vibrations induced by railway traffic: In-situ measurements and validation of a 2.5D FEM-BEM model. Soil Dyn. Earthq. Eng. **32**(1), 111–128 (2012)

Alves Costa, P., Colaço, A., Calçada, R., Cardoso, A.S.: Critical speed of railway tracks. Detailed and simplified approaches. Transport. Geotech. **2**, 30–46 (2015)

Araújo, N. M. F.: High-speed trains on ballasted railway track: Dynamic stress field analysis."PhD Thesis, Universidade do Minho, Portugal (2011)

Bian, X., Cheng, C., Jiang, J., Chen, R., and Chen, Y.: Numerical analysis of soil vibrations due to trains moving at critical speed. Acta Geotech. 1–14 (2014)

Chang, C.S., Selig, E.T., Adegoke, C.W.: Geotrack model for railroad truck performance. J. Geotech. Eng. Div. **106**(11), 1201–1218 (1980)

Dareeju, B., Gallage, C., Ishikawa, T., Dhanasekar, M.: Effects of principal stress axis rotation on cyclic deformation characteristics of rail track subgrade materials. Soils Found. **57**(3), 423–438 (2017)

El Kacimi, A., Woodward, P.K., Laghrouche, O., Medero, G.: Time domain 3D finite element modelling of train-induced vibration at high speed. Comput. Struct. **118**, 66–73 (2013)

Galavi, V., Brinkgreve, R. B. J.: Finite element modelling of geotechnical structures subjected to moving loads. In: Hicks et al. (ed.) VIII ECNUMGE - Numerical Methods in Geotechnical Engineering, pp. 235–240 . Taylor and Francis - Balkema, Delft, Netherlands (2014)

Gräbe, P., Clayton, C.: Effects of principal stress rotation on permanent deformation in rail track foundations. J. Geotech. Geoenviron. Eng. **135**(4), 555–565 (2009)

Huang, Y.H., Rose, J.G., Khoury, C.J.: Thickness design for hot-mix asphalt railroad trackbeds. Ann. J. AAPT, Misc. **56**(87), 427–453 (1987)

Inam, A., Ishikawa, T., Miura, S.: Effect of principal stress axis rotation on cyclic plastic deformation characteristics of unsaturated base course material. Soils Found. **52**(3), 465–480 (2012)

Ju, S.H., Ni, S.H.: Determining Rayleigh damping parameters of soils for finite element analysis. Int. J. Numer. Anal. Meth. Geomech. **31**(10), 1239–1255 (2007)

Kouroussis, G., Verlinden, O., Conti, C.: Finite-dynamic model for infinite media: corrected solution of viscous boundary efficiency. J. Eng. Mech. **137**(7), 509–511 (2011a)

Kouroussis, G., Verlinden, O., Conti, C.: Free field vibrations caused by high-speed lines: measurement and time domain simulation. Soil Dyn Earthq Eng **31**(4), 692–707 (2011b)

Krylov, V. V., Dawson, A. R., Heelis, M. E., Collop, A. C.: Rail movement and ground waves caused by high-speed trains approaching track-soil critical velocities. Proc. Instit. Mech. Eng., Part F: J. Rail Rapid Transit. 107–116 (2000)

Li, D.: Railway track granular layer thickness design based on subgrade performance under repeated loading. Doctor of Phylosophy PhD Thesis, University of Massachusetts, Amherst, Massachusetts, USA (1994)

Li, D., Selig, E.T.: Resilient modulus for fine-grained subgrade soils. J. Geotech. Eng. **120**(6), 939–957 (1994)

Madshus, C., Kaynia, A.M.: High-speed railway lines on soft ground: Dynamic behaviour at critical train speed. J. Sound Vib **231**(3), 689–701 (2000)

Mezeh, R., Mroueh, H., Hosseingholian, M., Sadek, M.: Fully-coupled numerical model for ballasted track analysis–Field measurements and predictions. Transp. Geotech. **27**, 100483 (2021)

MIDAS IT. Co. Ltd.: Manual of GTS-NX 2013 v1.2: new experience of geotechnical analysis system. MIDAS Company Limited, South Korea (2013)

Powrie, W., Yang, L. A., Clayton, C. R. I.: Stress changes in the ground below ballasted railway track during train passage. Proc. Instit. Mech. Eng. F J. Rail Rapid Transit. **221**(2), 247–261 (2007)

Qian, J., Du, Z., Lu, X., Gu, X., Huang, M.: Effects of principal stress rotation on stress–strain behaviors of saturated clay under traffic–load–induced stress path. Soils Found. **59**(1), 41–55 (2019)

Sayeed, M.A., Shahin, M.A.: Investigation into Impact of Train Speed for Behavior of Ballasted Railway Track Foundations. Proc. Eng. **143**, 1152–1159 (2016a)

Sayeed, M.A., Shahin, M.A.: Three-dimensional numerical modelling of ballasted railway track foundations for high-speed trains with special reference to critical speed. Transp. Geotech. **6**, 55–65 (2016b)

Sayeed, M.A., Shahin, M.A.: Design of ballasted railway track foundations using numerical modelling. Part I: Development. Can. Geotech. J. **55**(3), 353–368 (2018)

Shih, J.-Y., Thompson, D., Zervos, A.: The effect of boundary conditions, model size and damping models in the finite element modelling of a moving load on a track/ground system. Soil Dyn Earthq Eng **89**, 12–27 (2016)

Sun, Q., Indraratna, B., Grant, J.: Numerical Simulation of the Dynamic Response of Ballasted Track Overlying a Tire-Reinforced Capping Layer. Front. Built Environ. **6**, 1–15 (2020)

Takemiya, H.: Simulation of track-ground vibrations due to a high-speed train: the case of X-2000 at Ledsgard. J. Sound Vib **261**(3), 503–526 (2003)

Wang, H., Zeng, L.-L., Bian, X., Hong, Z.-S.: Train moving load-induced vertical superimposed stress at ballasted railway tracks. Adv. Civil Eng. (2020).

Xu, F., Yang, Q., Liu, W., Leng, W., Nie, R., Mei, H.: Dynamic Stress of Subgrade Bed Layers Subjected to Train Vehicles with Large Axle Loads. Shock. Vib. **2018**, 2916096 (2018)

Yang, L., Powrie, W., Priest, J.A.: Dynamic stress analysis of a ballasted railway track bed during train passage. J. Geotech. Geoenviron. Eng. **135**(5), 680–689 (2009)

Publisher's Note Springer Nature remains neutral with regard to jurisdictional claims in published maps and institutional affiliations.